

Influence of post uniform tensile and bending properties on the crash behaviour of AHSS and press-hardening steel grades

P. Larour, H. Pauli, T. Kurz, T. Hebesberger.

*Forschung und Entwicklung Kaltband, voestalpine Stahl GmbH
voestalpine Straße 3, 4020 Linz, Austria*

patrick.larour@voestalpine.com

Abstract: The axial crash behaviour of dual phase DP800 and press-hardening steel grades phs-ultraform® is investigated in this contribution with focus on the crash folding capability. The post uniform tensile properties and bending capability yield accurate predictive information about the axial crash folding behaviour. The rupture stress at fracture is an appropriate parameter for local ductility and crash folding assessment, whereas fracture elongation is gauge length dependent and rather accounts for average strain measurements. Some experimental illustrations are given for an optimised DP800 dual phase as well as tempered press-hardening phs-ultraform® steels. Improvement in the crash folding properties can be significantly related to post uniform tensile and bending properties.

Key words: post uniform tensile properties, bending test, crash folding behaviour, AHSS, phs-ultraform®.

1 INTRODUCTION

This study is dedicated to investigating how efficiently crash behaviour can be predicted based on small-scale trials. Tensile tests are usually used to characterise mechanical parameters. Some useful post uniform properties can be assessed when considering strength properties rather than elongation properties, which means rupture stress versus tensile strength rather than fracture elongation versus uniform elongation [Walp, 2007], [Schleich *et al.*, 2008], [Röcker, 2008]. Fracture elongation is unfortunately gauge length dependent and cannot account for local ductility behaviour, unless the gauge length is infinitely small [Röcker, 2008]. Local optical strain measurement would yield better results in assessing local true ductility in the post uniform necking zone [Röcker, 2008]. Other testing methods, such as bending tests, are useful in order to more efficiently predict, for example, bending-dominated failure that occurs with AHSS steel grades during folding/bending in axial and side crash tests [Walp, 2007], [Link *et al.*, 2008], [Dykeman *et al.*, 2009]. For press-hardening steels, the effect of annealing is demonstrated more effectively and with less relative scattering by the results of a bending test rather than by tensile elongation properties [Faderl *et al.*, 2009],

[Labudde *et al.*, 2009]. The bending angle at maximum load is a good indicator of the axial crash folding ability [Faderl *et al.*, 2009], [Laumann *et al.*, 2008], [Kurz *et al.*, 2009].

2 EXPERIMENTAL SET UP

2.1 Sample materials

A 1.2mm thick hot dip galvanized dual phase steel DP800 has been investigated, before and after metallurgical optimisation process as reported in [Pichler *et al.*, 2007] and [Hebesberger *et al.*, 2008]. The serial production of DP800 at voestalpine Stahl is performed only with the optimised version.

Hot dip galvanised press-hardening phs-ultraform® steels have been also investigated in the thickness range 1.5 to 2.0mm, in the hardened and tempered conditions (300°C to 500°C), as already referred in [Laumann *et al.*, 2008] and [Faderl *et al.*, 2009].

2.2 Tensile tests

The post uniform properties give an indication about remaining ductility after the onset of necking. This information can be used in order to correlate tensile properties with subsequent crash behaviour [Schleich *et al.*, 2007]. Following concepts can be found in literature data in order to characterise the post uniform ductility properties:

$$\varepsilon_{\text{postuniform}} = \ln\left(\frac{R_m}{R_b}\right) \quad [\text{Schleich } et al., 2008] \quad (1)$$

$$\Delta R/R = \frac{R_m - R_b}{R_b} \quad [\text{Röcker, 2008}] \quad (2)$$

$$\Delta R \cdot \Delta A = (R_m - R_b) \cdot (A - A_g) \quad [\text{Röcker, 2008}] \quad (3)$$

$$\text{CFS} = -\ln\left(\frac{R_b}{R_m} \cdot \left(1 - \frac{A_g}{2}\right)\right) \quad [\text{Walp, 2007}], [\text{VDI, 2007}] \quad (4)$$

[Yeh *et al.*, 1999]

$$D_{V_{\text{postuniform}}} = \sqrt{\left(\left[\ln\left(\frac{R_m}{R_b}\right)\right]^2 + \left[\ln\left(\frac{A - A_g + 1}{A_g + 1}\right)\right]^2\right)} \quad [\text{Schleich } et al., 2008] \quad (5)$$

With R_m : (ultimate) tensile strength, R_b : rupture stress (breaking strength) at sample fracture, A_g : uniform elongation; A : fracture elongation for a 80mm gauge length.

$\varepsilon_{\text{post uniform}}$ describes a fictive logarithmic post uniform elongation based on the ratio of tensile strength to rupture stress. $\Delta R/R$ represents the relative strength decrease between necking and fracture. CFS represents the critical true fracture strain in thickness direction. $D_{V_{\text{post uniform}}}$ criterion mixes post uniform strength and elongation. $\Delta R \cdot \Delta A$ estimates the energy absorption in the post uniform area. Criteria (1), (2), (4) do not consider fracture elongation,

which may help in case of high relative scattering as this is generally the case for UHSS steels grades.

2.3 Wedge bending tests

3 point wedge bending tests are conducted at voestalpine Stahl (Figure 1) and performed to a great extent in conformity with ISO 7438:2005 [ISO 7438, 2005]. Similar bending test set ups are described in [Walp, 2007], [Konieczny *et al.*, 2008] and [Link *et al.*, 2008].

Free rotating rollers with a radius R of 15 mm are used as shoulders without lubricant and are separated by twice the sheet thickness t . Milled bending sample which measures 60×60 mm are tested with a sharp bending punch with a 0.2mm radius R_1 . Such an instrument-monitored bending test provides a load-displacement curve depending on the immersion depth δ of the bending punch. Sample failure occurs in the maximum load range. After reaching the maximum load, the test is not interrupted but is performed until the defined punch stroke is reached. After reaching a bending angle of around 160°, which is dependent on the sheet thickness, the required load increases again because the punch is countered by the support rolls.

The recorded bending load/displacement curve is used to calculate the bending load/bending angle curve. The parameter typically used for this calculation is the bending angle at maximum load (Figure 1). This simplifies the following analysis of the resulting data. The bending angle of the specimen is not measured in the unloaded condition. The test is performed until full punch stroke, without being shut off at maximum load by a load device control.

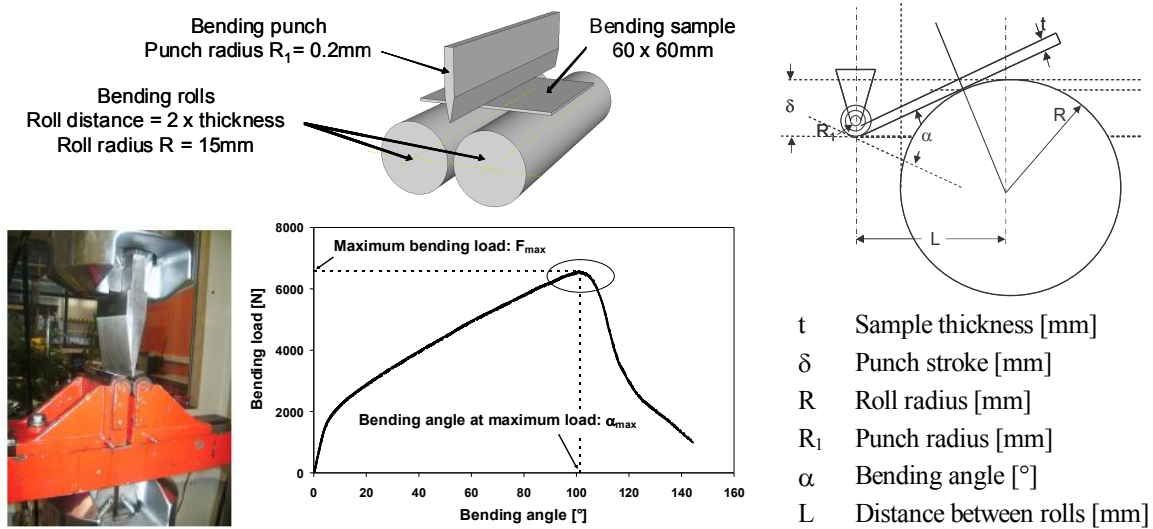


Figure 1: Device for instrumented 3 point wedge bending test at voestalpine Stahl.

2.4 Crash tests

Experimental set-up: voestalpine Stahl operates a horizontal crash unit to perform axial and bending crash tests on components (Figure 2a). The load is measured with a calibrated strain gage load measurement system on the crash plate behind the sample. The crash deformation of the sample is optically measured by means of a contrast grid device. Mean load and energy absorption are measured based on load/displacement measurement data (Figure 2b). The bending/buckling crash behaviour as well as the lightweight capability of AHSS steels can be assessed with such crash tests.

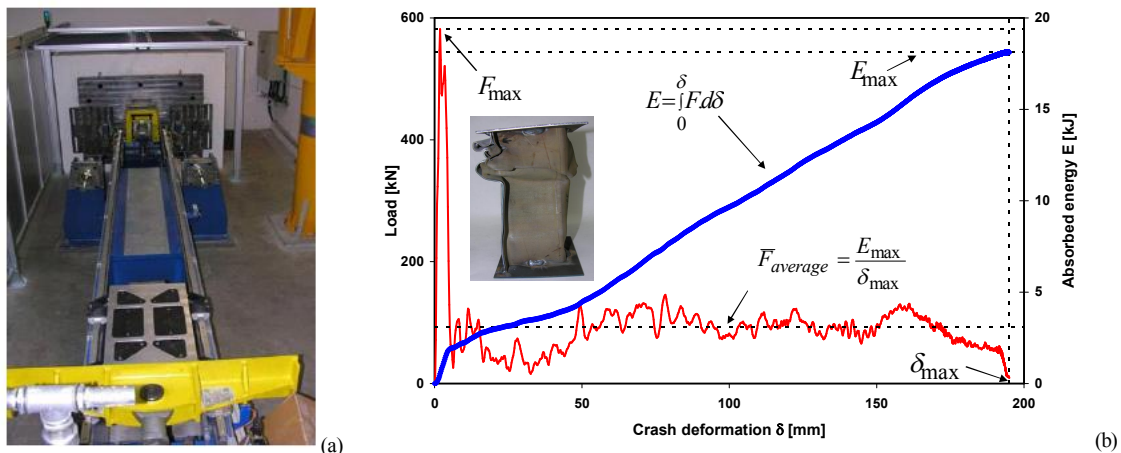


Figure 2: (a): Crash test set-up; (b): Load/displacement/energy curve in the axial crash.

Crash index: A crash index has been developed in order to quantify the axial crash folding ability (Figure 3). The crash folding behaviour is estimated based on the crack length similar to the methodology proposed in [Walp, 2007].

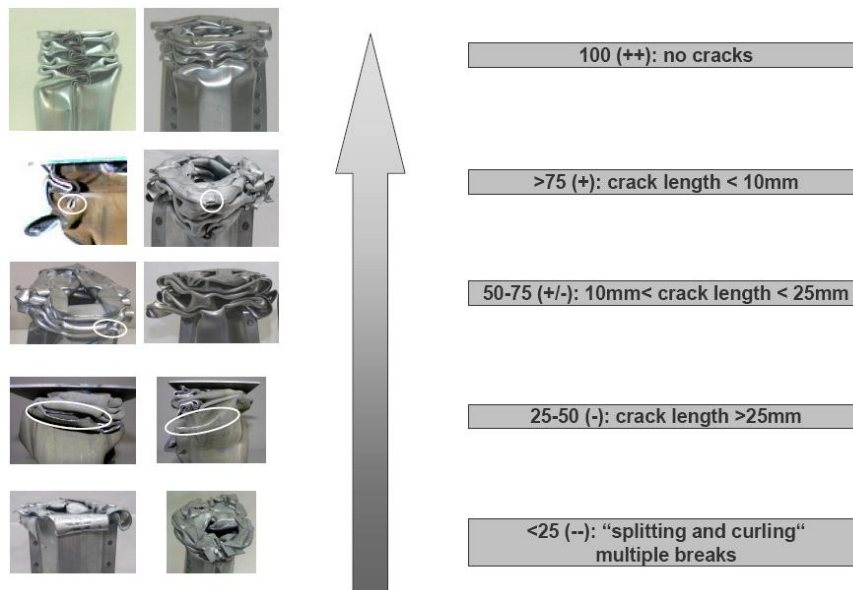


Figure 3: Crash index definition (axial crash folding behaviour).

Crash samples: Double hat and single hat crash box geometries have been used for DP800 and press-hardening steels respectively (Figure 4). Both geometries are spot welded with a 30mm pitch. No triggers have been used. Double hat crash boxes out of DP800 steel have been formed in a bending press. Single hat crash boxes out of phs-ultraform®, with the same geometry as described in [Laumann *et al.*, 2008], have been cold drawn, austenitised in a continuous furnace and hardened in a cooled shell die inside a press. The hardened and partially annealed hat-shaped sections are closed with a cover sheet of non-hardened phs-ultraform® with the same thickness that is spot welded on. The single hat-shaped sections are provided with head plates that are fillet-welded onto the ends.

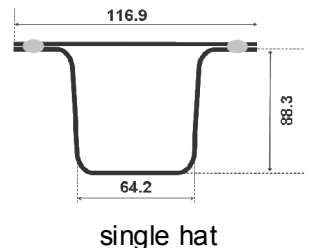
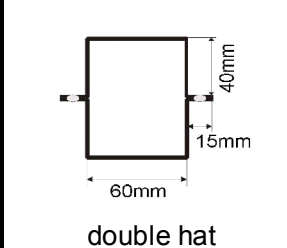
Steel grade	phs-ultraform®	DP800
Thickness (mm)	1.5 / 2.0	1.2
Impactor weight (kg)	268	126
Impact speed (kmh)	41	30-60
Weld pitch (mm)	30	30
Sample height (mm)	400	450
Triggers	no	no
Manufacturing	Cold deep drawing + quenched + tempered	Bending press
Head plates	yes	no
Crash box geometry	 single hat	 double hat

Figure 4: Crash box geometries and testing parameters.

3 EXPERIMENTAL RESULTS

3.1 Optimised DP800 steel grade

A dual phase DP800 steel grade from voestalpine Stahl has been optimised for serial production towards a better post uniform tensile ductility (Figure 5, Figure 7), bending ability (Figure 6) as well as crash folding ability (Figure 7). The metallurgical optimisation process of DP800 steel grade has been reported in [Pichler *et al.*, 2007] and [Hebesberger *et al.*, 2008]. The post uniform ductility (A_{80-Ag}) does not change significantly after DP800 steel optimisation. The post uniform strength decrease (R_m-R_b) however is much more significantly marked (Figure 5). The maximum bending angle increases with the optimised DP800 steel grade (Figure 6). The crash folding behaviour is also significantly improved (Figure 6, Figure 7) with a transition from multiple crash folding breaks (crash index: 20) into a better crash folding behaviour (crash index: 85). Figure 7 shows that all post uniform tensile

properties increase for the optimised DP800 steel grade. Post uniform criteria, which are postulated based on the ratio or difference of tensile strength R_m with rupture stress R_b , are therefore suitable to characterise the optimisation process of DP800 steel grade.

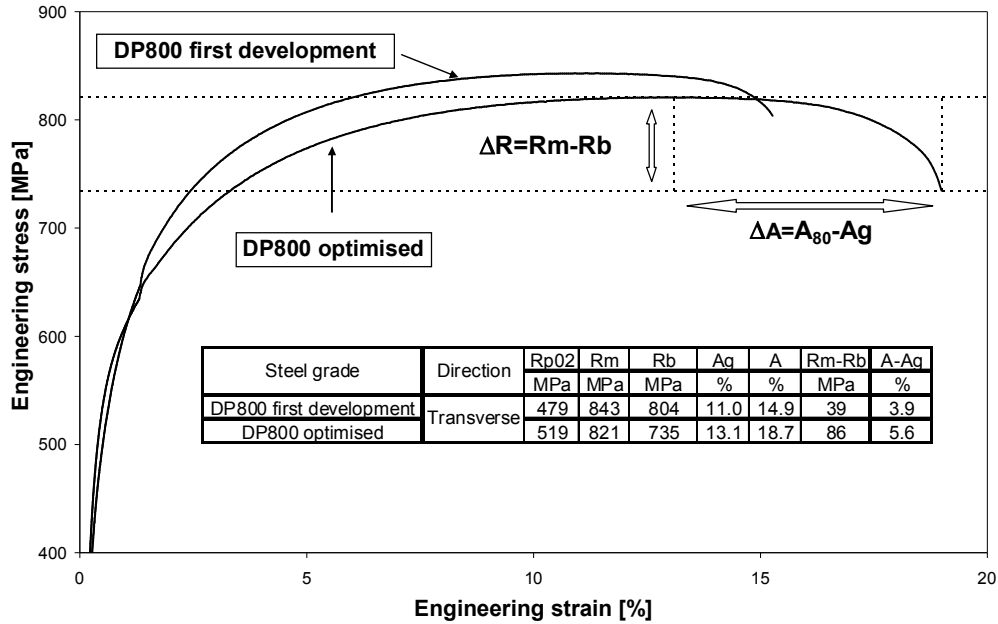


Figure 5: Transverse tensile stress-strain curves, post uniform properties, DP800.

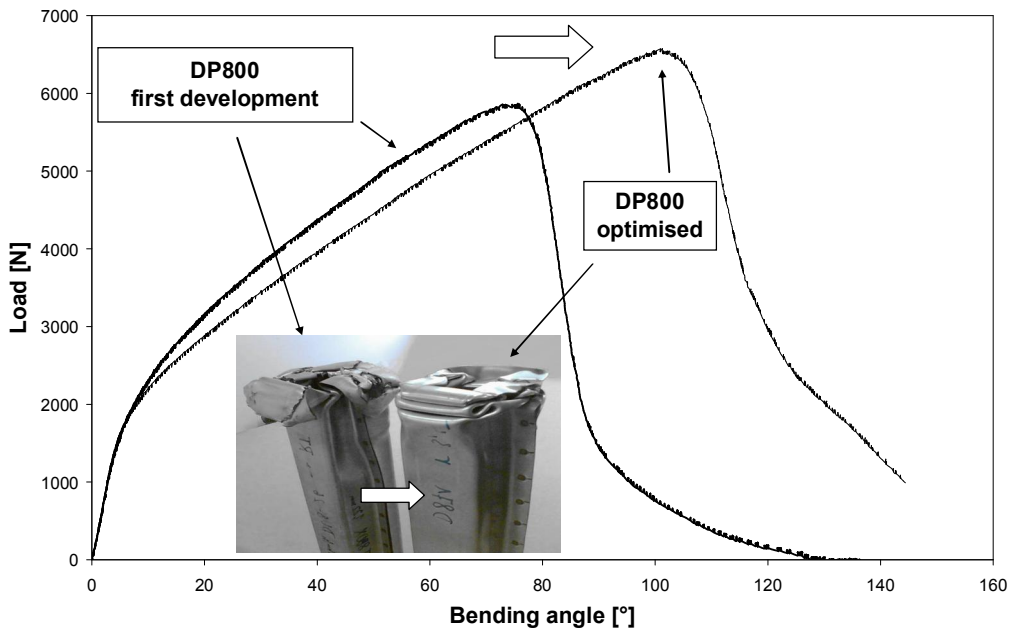


Figure 6: Longitudinal bending curves and crash properties, DP800.

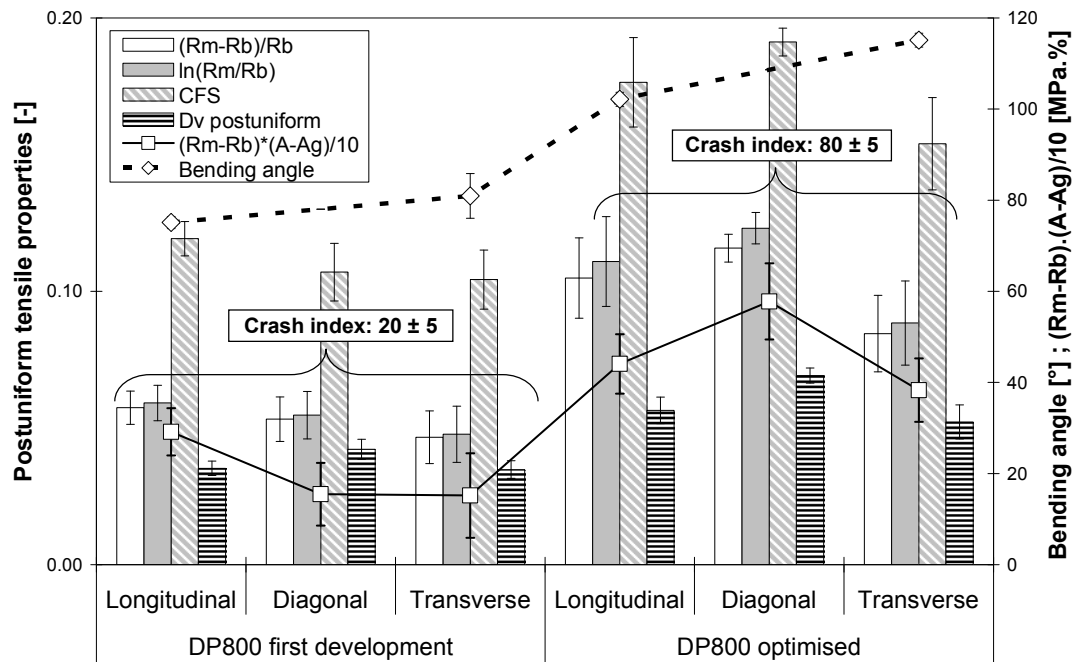


Figure 7: Post uniform tensile, bending and crash properties, DP800.

3.2 Tempered press-hardening steel grade

Tensile, bending and axial crash tests were conducted on the phs-ultraform® steel grade, both in the original quenched hardened condition and after being tempered at temperatures between 300°C and 500°C (for both 5 and 10 minutes) [Kurz *et al.*, 2009].

Tensile strength decreases significantly as the tempering temperature is increased, especially above 300°C (Figure 8). Fracture elongation increases only slightly with heat treatment, with a relatively high relative test scattering, so that such ductility increase cannot be reliably reproduced in individual samples (Figure 8). This problem has already been discussed in [Labudde *et al.*, 2009].

In contrast to fracture elongation, the bending angle significantly increases above 300°C, indicating a higher resistance to damage (Figure 8). This coincides with available literature data [Laumann *et al.*, 2008], [Labudde *et al.*, 2009]. Whereas quenched as well as quenched and 300°C tempered samples fully break apart in bending tests already after maximum load, the bending samples at higher tempering temperature show only some micro-cracks, but do not break apart during the test (Figure 9).

When considering the previously defined post uniform tensile properties, some similar results as for DP800 steel grades can be obtained for phs-ultraform® steel grade. The post uniform tensile properties increase steadily with increasing tempering temperature (Figure 10). The scattering of such tensile post uniform properties is also relatively small.

The crash folding behaviour, as quantified by the crash index, improves continuously as annealing temperature increases (Figure 10). “Splitting and curling” failure occurs in the hardened condition, which results in comparatively low energy absorption capacity in spite of

the high tensile strength of the base material. A defined crash folding deformation pattern occurs first at a tempering temperature of 300°C. This leads to more effective energy absorption and smaller crash deformation in spite of still existing crash fold breaks and moderate decrease in strength. The crash folding behaviour improves beginning at an annealing temperature of 400°C but this can no longer compensate for the loss in strength of the base material. The overall crash deformation increases again, and both energy absorption and mean load are reduced. The optimum annealing temperature with respect to energy absorption capacity ranges therefore between 300 and 400°C.

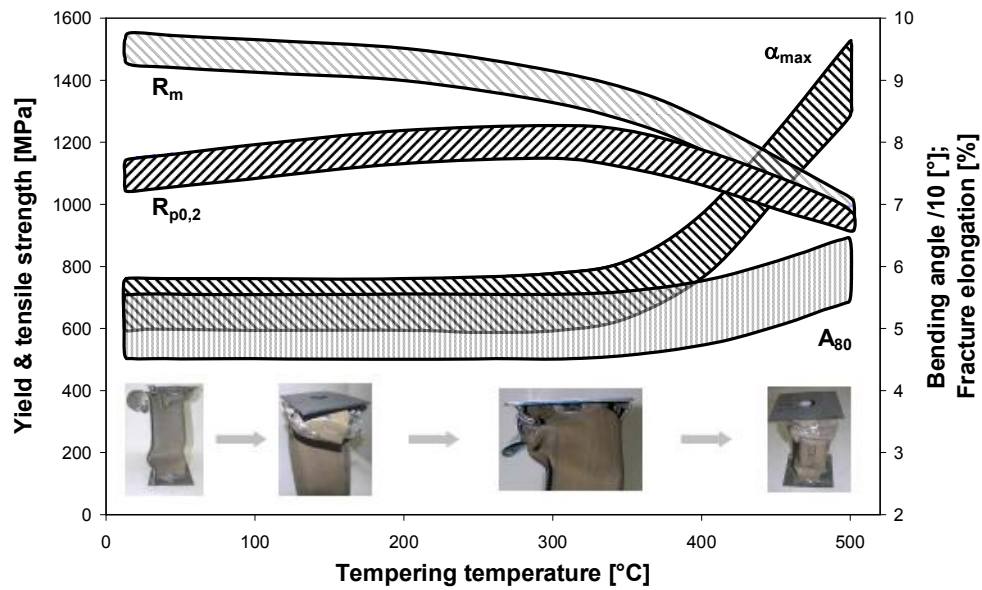


Figure 8: Longitudinal tensile and bending properties vs. tempering temperature *phs-ultraform*®.

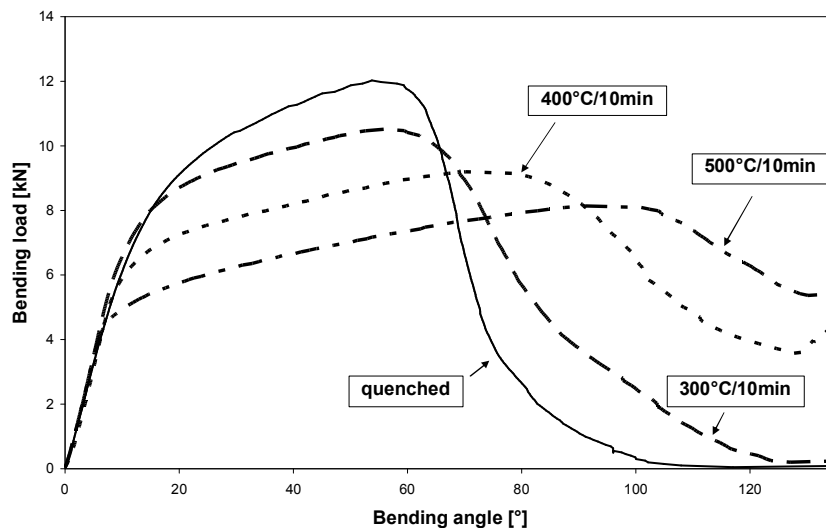


Figure 9: Longitudinal bending curves vs. tempering temperature, *phs-ultraform*®.

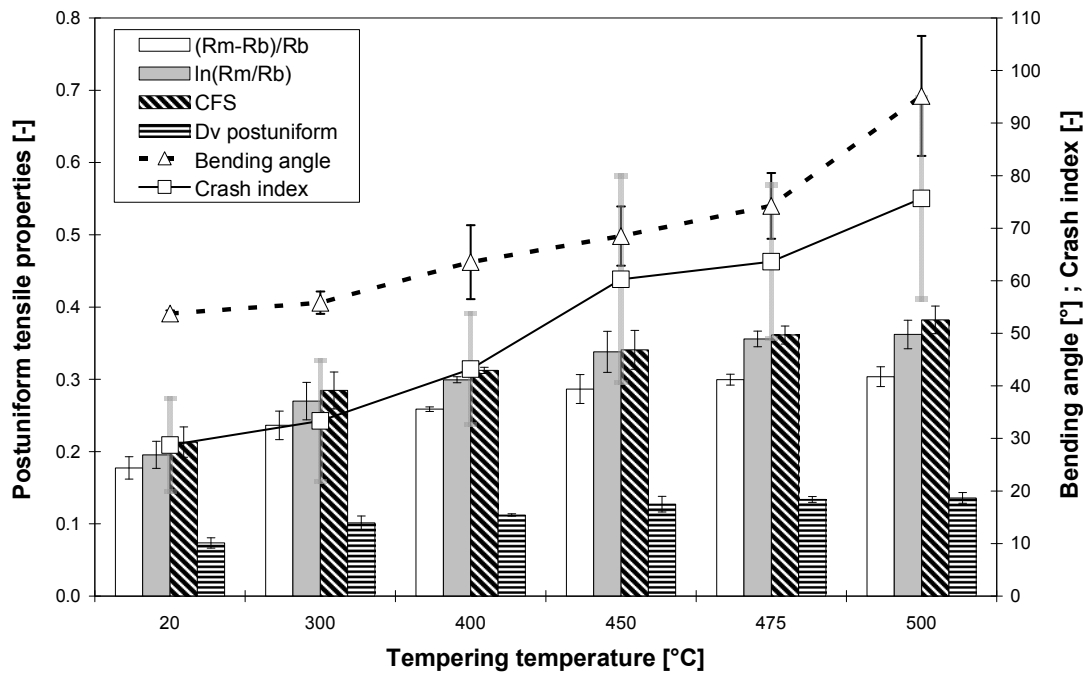


Figure 10: Longitudinal post uniform tensile, bending properties and crash index vs. tempering temperature, pbs-ultraform®.

4 CONCLUSIONS

The crash folding behaviour of dual phase DP800 and press-hardening pbs-ultraform® steel grades in axial crash condition can be well quantified by means of a crash index factor.

Fracture elongation, as determined in tensile tests as a characteristic variable of material ductility, is not quite suitable in order to predicting the axial crash folding behaviour. There is a correlation between crash behaviour and fracture elongation; however, the high relative scattering of fracture elongation values for UHSS steels overshadows the adequate interpretation of such results.

Modified tensile post uniform criteria based on rupture stress rather than fracture elongation deliver much better predictive results with regard to crash folding capability and with less relative scattering as for fracture elongation.

The bending test has also proven to be quite suitable for crash folding prediction, as a result of its relatively small variation results. This was demonstrated by a comparison of statistical analyses of numerous crash tests with the corresponding bending angle at maximum load.

5 REFERENCES

- [**Dykeman et al., 2009**] Dykeman, J.; Hoydick, D.; Link, T.; Mitsuji, H.; “Material Property and Formability Characterization of Various Types of High Strength Dual Phase Steel”; SAE Technical Paper 2009-01-0794.
- [**Faderl et al., 2009**] Faderl, J.; Kolnberger, S.; Kurz, T.; Luckeneder, G.; Manzenreiter, T.; Rosner, M.; “phs-ultraform[®] - Continuous galvanizing meets press-hardening”; CHS² Luleå Schweden (2009) pp. 283-292.
- [**Hebesberger et al., 2008**] Hebesberger, T.; Pichler, A.; Pauli, H.; Ritsche, S.; “Dual-phase and complex-phase: AHSS Material for a wide range of application”; Proc. Conf. on Steels in Cars and Trucks Wiesbaden (2008) pp. 456-463.
- [**ISO 7438, 2005**] DIN EN ISO 7438:2005 Norm; „Metallische Werkstoffe-Biegeversuch“.
- [**Konieczny, 2008**] Konieczny, A.A.; „On the Formability Behavior of Advanced High Strength Steels”; Steel Research Int. 79/1 (2008) pp. 47-54.
- [**Kurz et al., 2009**] Kurz, T.; Larour, P.; Till, E. T.; “Crashperformance und Duktilität von presshärtenden Stählen – reicht der Zugversuch zur Beschreibung?”; Proc. Conf. 4. Erlanger Workshop Warmblechumformung (2009).
- [**Labudde et al., 2009**] Labudde, Th.; Bleck, W.; “Formability characterisation of press hardened steels”; CHS² Luleå Schweden (2009) pp. 127-135.
- [**Laumann et al., 2008**] Laumann, T.; Pfestorf, M.; “Crash behaviour of various modern steels exposed to high deformation rates”; Steel Grips 6. CHS² (2008) pp. 143-151.
- [**Link et al., 2008**] Link, T.M.; “Effects of Paint Baking on the Axial Crash Performance of Advanced High Strength Steels”; MS&T 2008, Pittsburgh, pp. 1989-2000.
- [**Pichler et al., 2007**] Pichler, A.; Traint, S.; Hebesberger, T.; Stiaszny, P.; Werner, E.A.; „Processing of thin sheet multiphase steel grades“; Steel Research International 78/3 (2007) pp. 216-223.
- [**Röcker, 2008**] Röcker, O.; “Untersuchungen zur Anwendung hoch- und höchstfester Stähle für walzprofilierte Fahrzeugstrukturkomponenten“; PhD Berlin (2008) pp. 63-66.
- [**Schleich et al., 2007**] Schleich, R.; Sindel, M.; Liewald, M.; “Potentials of new ductility criterions in car development with lightweight materials“; International Journal of Aluminium 3/2007, pp. 80-82.
- [**Schleich et al., 2008**] Schleich, R.; Sindel, M.; Keith, T.; Liewald, M.; “Neue Duktilitätskriterien für die Qualitätsbewertung von Leichtbauwerkstoffen“; MP Materials Testing 50/9 (2008) pp. 472-476.
- [**VDI, 2007**] VDI: „Mechanische Eigenschaften“; In: Anwendungstechnologie Aluminium Edition 2. ISBN 978-3-540-69451-9 (Online) (2007) pp. 279-398.
- [**Walp, 2007**] Walp, M.S.; “Impact Dependent Properties of Advanced and Ultra High Strength Steels”; SAE Technical Paper 2007-01-0342.
- [**Yeh et al., 1999**] Yeh, J.R.; Summe, T.L.; Seksaria, D.C.; “The Development of an Aluminium Failure Model for Crashworthiness Design”; In: AMD-Vol. 237/BED-Vol.45, ASME (1999) pp. 97-105.